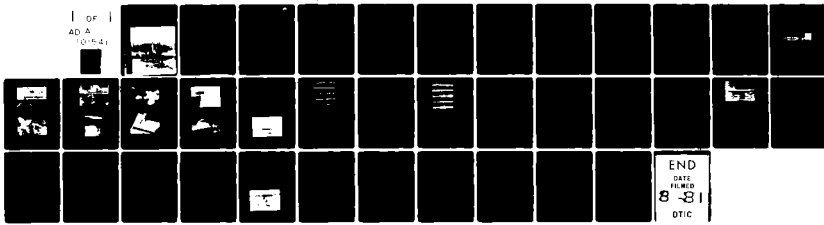


AD-A101 541 COLD REGIONS RESEARCH AND ENGINEERING LAB HANOVER NH F/G 20/11
VIBRATIONS CAUSED BY SHIP TRAFFIC ON AN ICE-COVERED WATERWAY, (U)
APR 81 F D HAYNES, M MAEAETAEMEN NCE-1A-79-026

UNCLASSIFIED CRREL-81-5 NL

1 OF 1
AD A
(0-5-4)



END
DATE FILMED
8-81
DTIC

CRREL
REPORT 81-5

JUL 17 1981

A



Vibrations caused by ship traffic on an
ice-covered waterway

AD A101541

DMG FILE COPY



For conversion of SI metric units to U.S. British customary units of measurement consult ASTM Standard E380, Metric Practice Guide, published by the American Society for Testing and Materials, 1916 Race St., Philadelphia, Pa. 19103.

Cover: USCGC Mackinaw upbound on the St. Marys River, Michigan.

CRREL Report 81-5



Vibrations caused by ship traffic on an ice-covered waterway

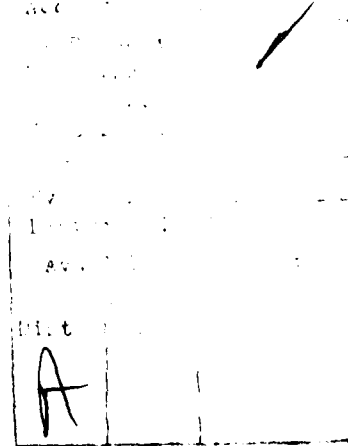
F.D. Haynes and M. Määtänen

April 1981

Prepared for
U.S. ARMY ENGINEER DISTRICT, DETROIT
By

UNITED STATES ARMY CORPS OF ENGINEERS
COLD REGIONS RESEARCH AND ENGINEERING LABORATORY
HANOVER, NEW HAMPSHIRE, U.S.A.

Approved for public release, distribution unlimited



Unclassified

~~SECURITY~~ CLASSIFICATION OF THIS PAGE (When Data Entered)

DD FORM 1 JAN 73 1473 EDITION OF 1 NOV 68 IS OBSOLETE

Unclassified

SECURITY CLASSIFICATION OF THIS PAGE (When Data Entered)

037100

20. Abstract (cont'd).

on the shore and are related to icebreaking by the bow. Vibration magnitudes are dependent upon the velocity of the ship, the energy expended by the ship, the cross-sectional area of the ship, weather, conditions of the ice and soil, and site-specific conditions. Further studies are needed to determine the effects of these factors and to determine the mode of energy transmission.

PREFACE

This report was prepared by F. Donald Haynes, Materials Research Engineer and Dr. Mauri Maattanen, University of Oulu, Finland, Visiting Research Engineer, Ice Engineering Research Branch, Experimental Engineering Division, U.S. Army Cold Regions Research and Engineering Laboratory. The study was conducted for the U.S. Army Engineer District, Detroit (NCE-IA-79-026, St. Marys River Vibration Study).

The authors express their appreciation to Dr. Donald Nevel and George Aitken for their technical review of the report and to John Kalafut and John Gagnon for their valuable assistance in the investigation. They also express appreciation to Charles Gordon and Ray Doran for permission to use their properties as test sites for data collection. Appreciation is also expressed to the U.S. Steel Corp. for permission to instrument the Cason J. Callaway.

The contents of the report are not to be used for advertising or promotional purposes. Citation of brand names does not constitute an official endorsement or approval of the use of such commercial products.

CONTENTS

	Page
Abstract	i
Preface	iii
Introduction	1
Test setup	1
Test results	8
The USCCC Mackinaw	8
The Roger Blough	10
The Cason J. Callaway	12
The Imperial St. Clair	15
Vibration levels	15
Discussion	19
Frequency content	19
Magnitude	20
Mode of transmission	23
Opening the channel	24
Flexural waves	24
Duration and occurrence of maximum vibrations	25
Effect of weather	25
Conclusions and recommendations	26
Literature cited	27

ILLUSTRATIONS

Figure

1. Location of test sites	2
2. Test sites on the St. Marys River	2
3. Vibration instrumentation layout	3
4. The Gordon site	3
5. The Doran site	4
6. Accelerometers mounted on the ice	4
7. Wire rope prevented loss of accelerometers during breakup	5
8. Hydrophone prior to placement in river under the ice	5
9. Array of geophones buried in the soil	6
10. Accelerometers mounted on floor joists at the Gordon site	6
11. Accelerometers mounted on the roof eave at the Doran site	7
12. Cason J. Callaway locking through at Sault Ste. Marie	7
13. USCCC Mackinaw passing upbound at the Gordon site	8
14. Signals of USCCC Mackinaw passing the Gordon site	9
15. Magnitude of vibrations as the USCCC Mackinaw passed the Gordon site upbound	9
16. Auto power spectrum plots for the geophone and accelerometer on the house for the Mackinaw upbound at the Gordon site	9
17. Auto power spectrum plots for the accelerometer on the ice and the geophone for the Mackinaw upbound at the Gordon site	10
18. Auto power spectrum plots for the accelerometer on the ice and the geophone for the Mackinaw upbound at the Gordon site	10

Figure	Page
19. Signals of <i>Roger Blough</i> passing the Gordon site	11
20. Auto power spectrum plot for the geophone mounted perpendicular to the channel for the <i>Roger Blough</i> downbound at the Gordon site	11
21. Auto power spectrum plot for the geophone mounted parallel to the channel for the <i>Roger Blough</i> downbound at the Gordon site	11
22. Auto power spectrum plot for the vertically mounted geophone for the <i>Roger Blough</i> downbound at the Gordon site	12
23. Magnitude of vibrations for the <i>Roger Blough</i> passing the Gordon site	12
24. Auto power spectrum plots for the transverse and longitudinal direction accelerometers on the bow of the <i>Cason J. Callaway</i> as it passed the Gordon site downbound	12
25. Auto power spectrum plots for the vertical accelerometers on the bow and stern of the <i>Cason J. Callaway</i> as it passed the Gordon site	12
26. Auto power spectrum plot for the geophone mounted perpendicular to the channel as the <i>Cason J. Callaway</i> passed the Gordon site downbound	13
27. Auto power spectrum plot for the geophone mounted parallel to the channel as the <i>Cason J. Callaway</i> passed the Gordon site downbound	13
28. Magnitude of vibrations for the <i>Cason J. Callaway</i> passing the Doran site downbound	13
29. Time record for the accelerometer mounted in the transverse direction on the bow of the <i>Cason J. Callaway</i>	13
30. Auto power spectrum for the accelerometer mounted in the transverse direction on the bow of the <i>Cason J. Callaway</i>	14
31. Time record for the accelerometer mounted in the longitudinal direction on the bow of the <i>Cason J. Callaway</i>	14
32. Auto power spectrum for the accelerometer mounted in the longitudinal direction on the bow of the <i>Cason J. Callaway</i>	14
33. Time record for the accelerometer mounted in the vertical direction on the bow of the <i>Cason J. Callaway</i>	14
34. Auto power spectrum for the accelerometer mounted in the vertical direction on the bow of the <i>Cason J. Callaway</i>	15
35. Auto power spectrum for the accelerometer mounted in the transverse direction on the stern of the <i>Cason J. Callaway</i>	15
36. Auto power spectrum for the accelerometer mounted in the longitudinal direction on the stern of the <i>Cason J. Callaway</i>	15
37. Auto power spectrum for the accelerometer mounted in the vertical direction on the stern of the <i>Cason J. Callaway</i>	15
38. <i>Imperial St. Clair</i> passing the Doran site downbound	16
39. Auto power spectrum for the accelerometer mounted perpendicular to the channel on the ice as the <i>Imperial St. Clair</i> passed the Doran site	16
40. Auto power spectrum for the accelerometer mounted perpendicular to the channel on the house as the <i>Imperial St. Clair</i> passed the Doran site	16
41. Coherence function for the accelerometers mounted perpendicular to the channel on the ice and house as the <i>Imperial St. Clair</i> passed the Doran site	16
42. Magnitude of vibrations as the <i>Imperial St. Clair</i> passed the Doran site downbound	17

Figure	Page
43. Magnitude of vibrations as the George Stinson passed the Gordon site downbound	17
44. Magnitude of vibrations as the USCGC Mackinaw passed the Gordon site upbound	17
45. Magnitude of vibrations as the USCGC Mackinaw passed the Doran site upbound	17
46. Magnitude of vibrations as the Roger Blough passed the Doran site upbound on 18 March 1979	18
47. Magnitude of vibrations as the Roger Blough passed the Doran site upbound on 24 February 1979	18
48. Magnitude of vibrations as the Philip Clarke passed the Doran site downbound on 10 February 1979	18
49. Magnitude of vibrations as the Philip Clarke passed the Doran site downbound on 21 March 1979	18
50. Magnitude of vibrations as the Philip Clarke passed the Gordon site downbound on 3 April 1979	19
51. Levels of vibration for seven ships passing the test sites	19
52. Auto power spectrum for the hydrophone as the Roger Blough passed the Doran site	19
53. Time record for the hydrophone as the Roger Blough passed the Gordon site	19
54. Auto power spectrum for the accelerometer mounted on the ice in the vertical direction as the USCGC Mackinaw passed the Gordon site upbound	21
55. Auto power spectrum for the geophone mounted in the vertical direction as the USCGC Mackinaw passed the Gordon site upbound	21
56. Accelerometers mounted on the ice, and shoreline crack	22
57. Seismic wave paths	23
58. Average daily temperature for 1 January through 10 April 1979, Sault Ste. Marie, Michigan	26

TABLES

Table

1. Comparison of vibrations with and without an ice cover	22
2. Comparison of vibrations with solid ice and broken ice	22

VIBRATIONS CAUSED BY SHIP TRAFFIC ON AN ICE-COVERED WATERWAY

F.D. Haynes and M. Määtänen

INTRODUCTION

During the 8-year demonstration program of the Great Lakes-St. Lawrence Seaway navigation season extension, several problems have been identified. One of these was vibrations on shore resulting from ship traffic. This was particularly noticeable on the St. Marys River south of Sault Ste. Marie, Michigan. Several people with homes along the shore complained of severe vibrations, especially when the ice was frozen solid and the soil between the shore and the house was frozen. An ice boom was installed about 2 miles upstream from the problem area in the winter of 1975-76 (Perham 1978) and it has mitigated the vibration problem to some degree.

In January 1979, transducers were placed on the ice, in the soil, and on houses at two sites on the St. Marys River. The objectives were 1) to positively identify the ships as the source of the vibrations, 2) to determine the magnitude, duration and frequency content of the vibrations, and 3) to determine the mode of transmission for the vibration signals. All transducer signals were recorded on tape and later analyzed with a strip chart recorder and a digital signal analyzer.

TEST SETUP

Figures 1 and 2 show the locations of the two test sites. The Gordon site was chosen because the residence is about 30 m from shore, and it is a good vantage point from which to view the ship traffic. At this site shoreline reinforcement is buried rock and timber. The Doran site was chosen because the shoreline protection is quite different: steel sheet piling driven about 1.3 m deep along the shore.

Figure 3 shows the general instrumentation layout. Three accelerometers were mounted on a steel plate that was tack welded to a pipe frozen into the ice sheet. The x and y direction accelerometers were oriented perpendicular to and parallel to the ship channel, respectively, while the z direction accelerometer was vertically oriented. Accelerometers mounted on the ice are shown in Figures 4 and 5. A close-up view of the accelerometer mounting on the ice is shown in Figure 6. A 6.35-mm wire rope is shown attached to the mounting plate. This wire rope was connected to a steel rod driven into the soil on shore. When the ice moved, the tack welds failed, separating the mounting plate from the

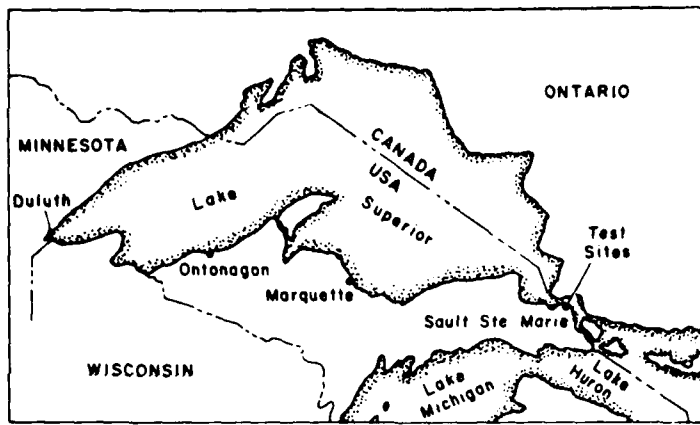


Figure 1. Location of test sites.

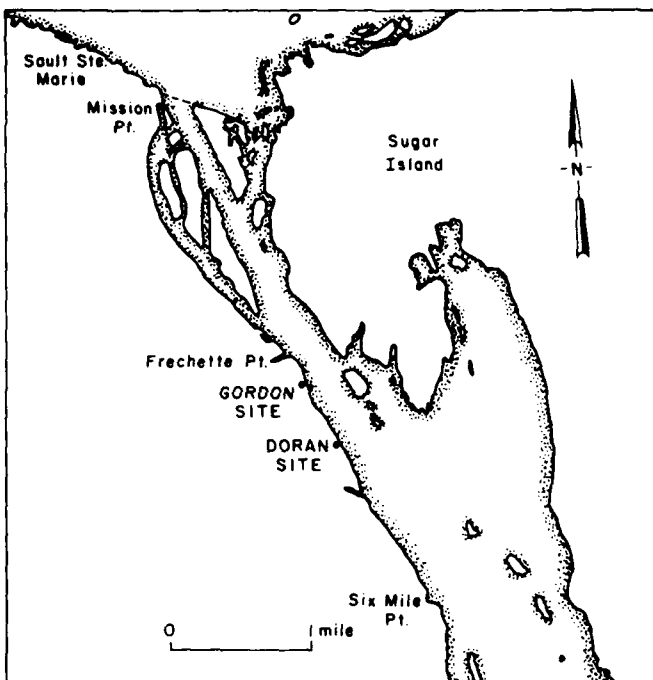


Figure 2. Test sites on the St. Marys River.

pipe. The wire rope acted as a fail-safe device which prevented the loss of the accelerometers. Figure 7 shows how the system worked during breakup.

At each site a hydrophone (Fig. 8) was placed at mid-depth in the water (about 1.3 m). About midway between the shore and the houses three 1-Hz geophones were buried about 0.15 m below the ground surface (Fig. 9). Good coupling be-

tween the geophones and the soil was achieved by placing a soil-water slurry around each geophone and allowing it to freeze overnight.

At the Gordon site, x, y and z direction accelerometers were mounted on the floor joints of the second floor of the house (Fig. 10). They were in about the same orientation as those mounted on the ice and were the same type. At the Doran site, x, y and z accelerometers were mounted on

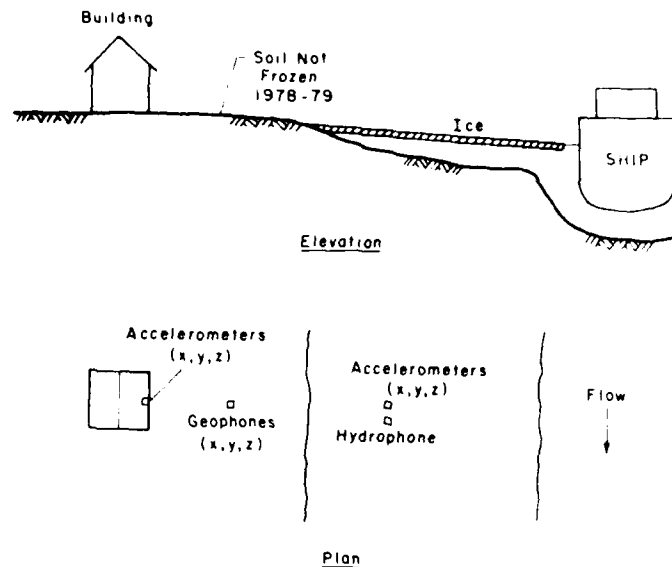


Figure 3. Vibration instrumentation layout.

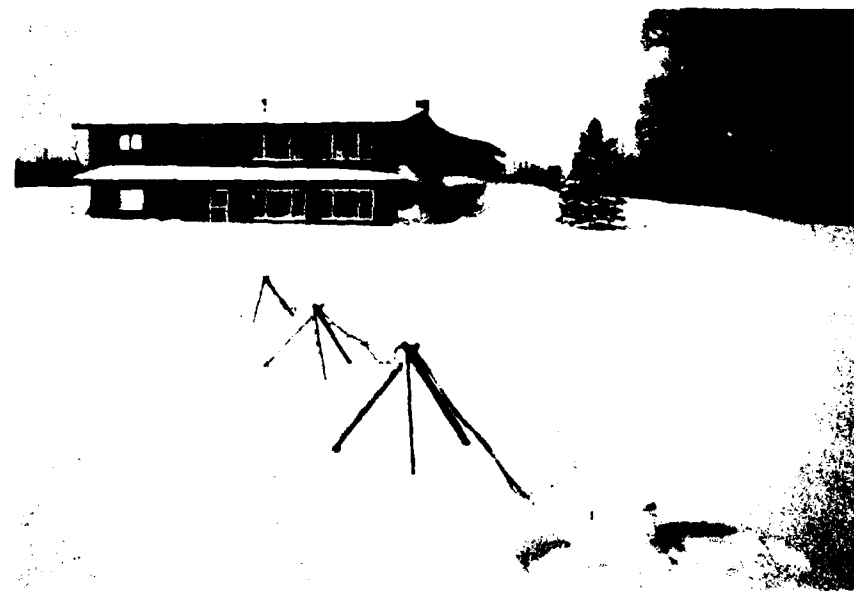


Figure 4. The Gordon site with the accelerometers on the ice under the white bucket in foreground.

the roof eave of the house (Fig. 11). These locations were chosen because they were readily accessible and permitted measurement of typical structural responses. All transducers were calibrated and data were collected on FM tape.

The name and velocity of each ship were ob-

served as a measure of traffic past the two sites. The velocity was found by selecting a marker across the channel and measuring the time elapsed between passage of bow and stern past the marker. After the name was recorded, the length of the ship was found in the *Great Lakes*



Figure 5. The Doran site with the accelerometers on the ice in the foreground



Figure 6. Accelerometers mounted on the ice with wire rope attached to the mounting plate.

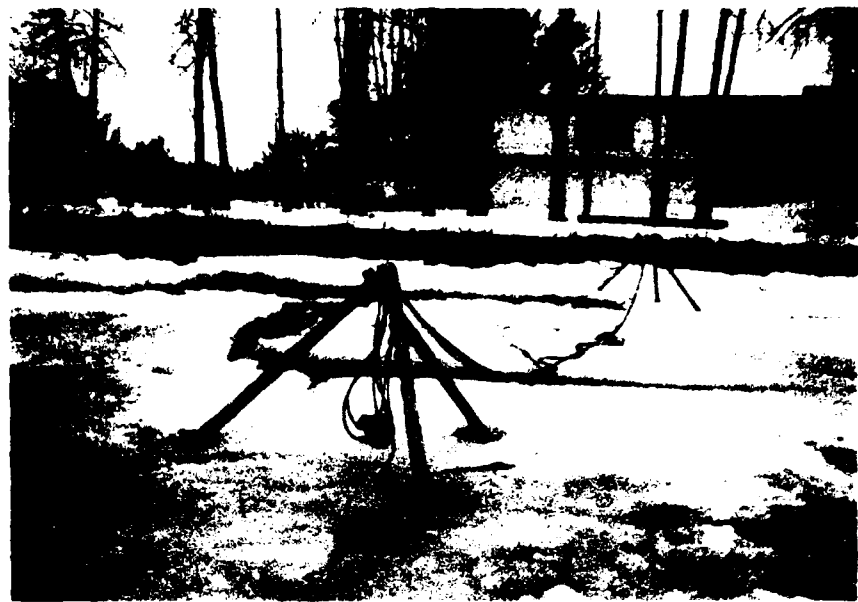


Figure 7. Wire rope prevented loss of accelerometers during breakup



Figure 8. Hydrophone prior to placement in river under the ice



Figure 9 - Array of geophones buried in the soil

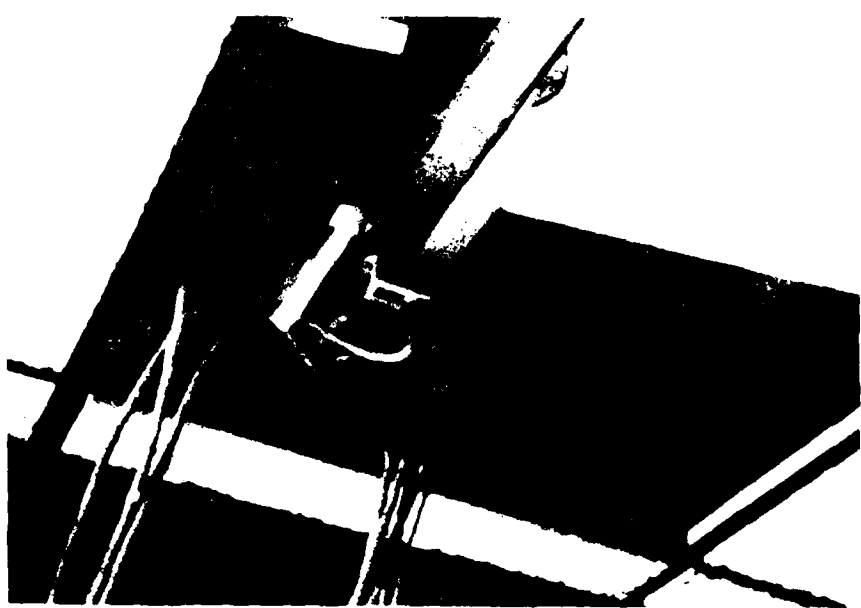


Figure 10 - Accelerometers mounted on floor joists at the Gordon site

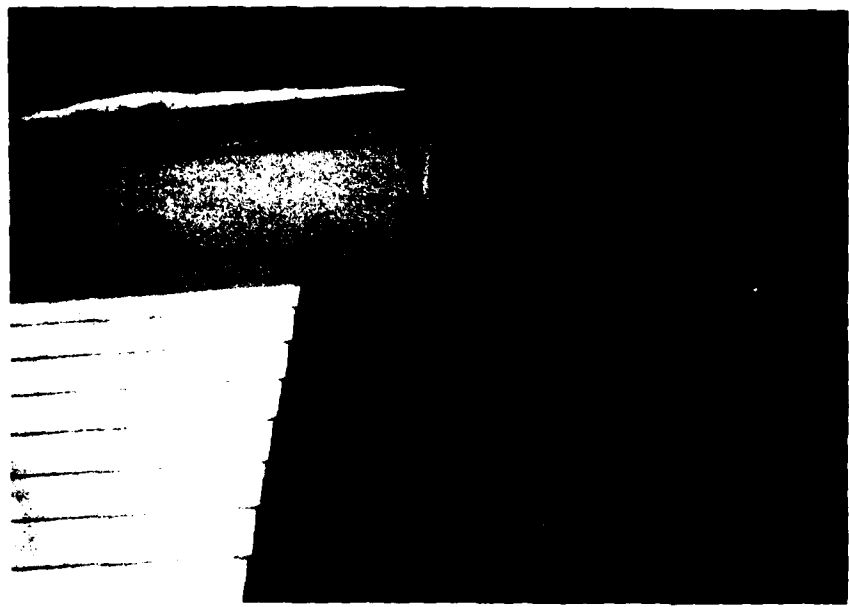


Figure 11. Accelerometers mounted on the roof eave at the Doran site.



Figure 12. Cason J. Callaway lock going through at Sault Ste. Marie.

Red Book (1979). Not all the ship traffic between January and April (the period of instrumentation) was recorded since manual operation of the recorder was necessary and the recorders were not always manned. However, 70 ship passages were recorded at the Gordon site and 30 at the Doran site, giving a good representation of the winter navigation season.

In order to identify the ships as the source of vibrations we requested and received the permission of U.S. Steel to instrument one of their ore carriers. The *Cason J. Callaway*, a 233-m (767-ft) by 21.3-m (70-ft) ship with a 5.22-MW (7,000-hp) engine was chosen (Fig. 12). Three accelerometers (*x*, *y* and *z* directions) were placed in the bow at the waterline and three more in the stern at the waterline while the ship was in dry dock at Duluth Harbor in December 1978. Data were collected on board ship using an instrumentation recorder like those used on shore.

TEST RESULTS

As mentioned in the previous section all data were recorded on FM tape. First, all tapes were played out on a strip chart recorder with a frequency response up to 125 Hz to identify particular areas of interest. Vibration magnitude and duration were identified from a strip chart recorder plot and frequency content was identified with a digital signal analyzer.

The USCGC Mackinaw

Figure 13 shows USCGC *Mackinaw* passing the Gordon site. Figure 14 is a plot of the data from the strip chart recorder for the *Mackinaw* passing the Gordon site on 20 January 1979. There were voice interrupts on channel no. 8 at the points where we observed that the bow and stern were passing the test site. The magnitudes of the transducer signals were found from Figure 14 and plotted on a standard vibration damage chart (Fig. 15). It can be seen from Figure 14 that these maximum signals were at 5 Hz, and that is how they were plotted in Figure 15. The 5-Hz frequency is the propeller noise of the *Mackinaw*, which had a four-bladed propeller operating at a shaft speed of 75 rpm. It is also evident in Figure 14 that a strong 5.5-Hz signal is present in all geophones.

For a check on the dominant frequency an HP Digital Signal Analyzer was used. This analyzer has a two-channel input so signals from two transducers can be compared. Figure 16 shows the auto power spectra for the *x*-direction geophone and the *x*-direction accelerometer on the house. The auto spectrum is the Fourier transform of the auto correlation function in the time domain. The dominant frequency for the geophone signal is 5.5 Hz. The resolution is 0.5 Hz on a 128-Hz bandwidth for the analyzer. Therefore the 5- to 5.5-Hz frequency obtained from the strip chart recorder is confirmed by the auto spectrum. There is good correlation at 5.5 Hz for



Figure 13. USCGC *Mackinaw* passing upbound at the Gordon site.

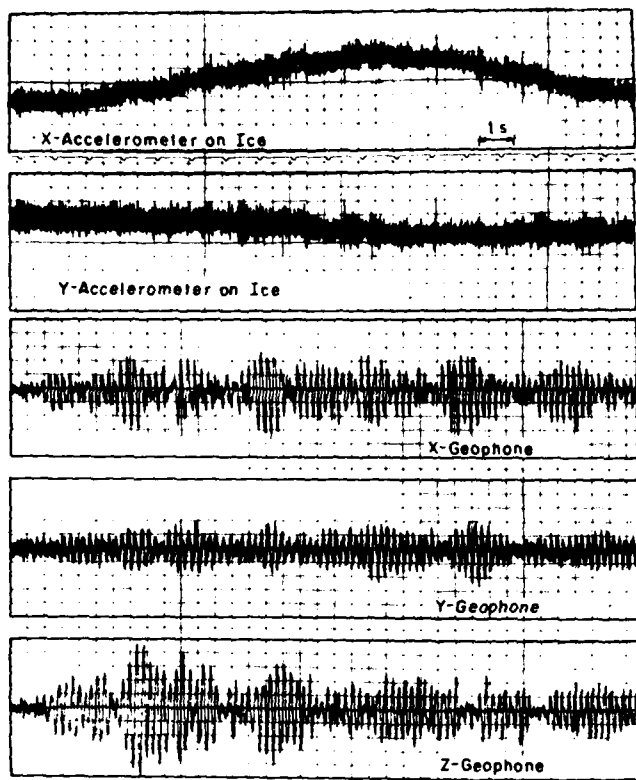


Figure 14. Signals of USCGC Mackinaw passing the Cordon site at 12.8 mph on 20 January 1979.

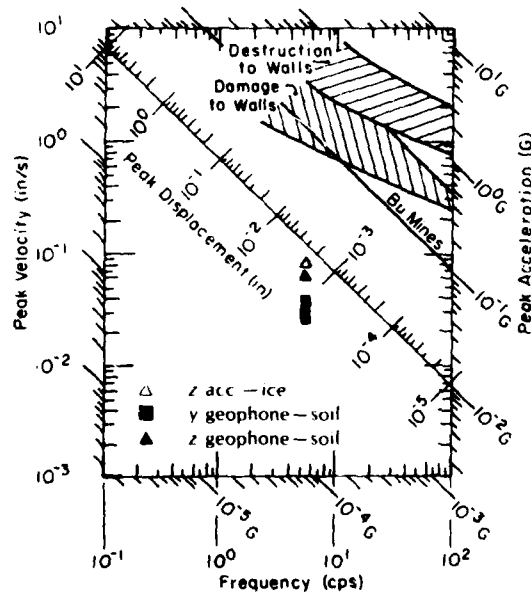


Figure 15. Magnitude of vibrations as the USCGC Mackinaw passed the Cordon site upbound on 20 January 1979 at 12.8 mph (x is perpendicular to and y is parallel to the ship channel; z is vertical).

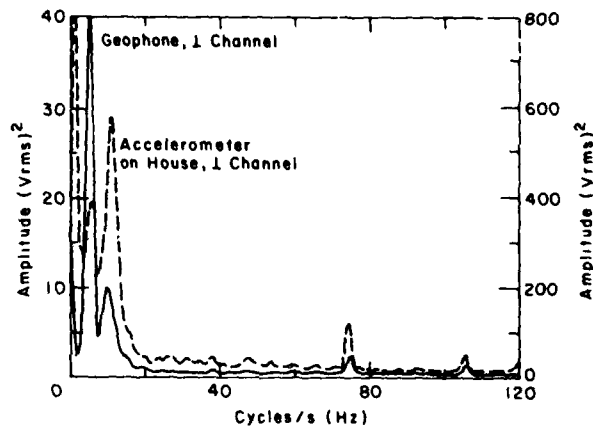


Figure 16. Auto power spectrum plots for the geophone and accelerometer on the house (both mounted perpendicular to the channel) for the Mackinaw upbound at the Cordon site. Right scale for accelerometer, left scale for geophone.

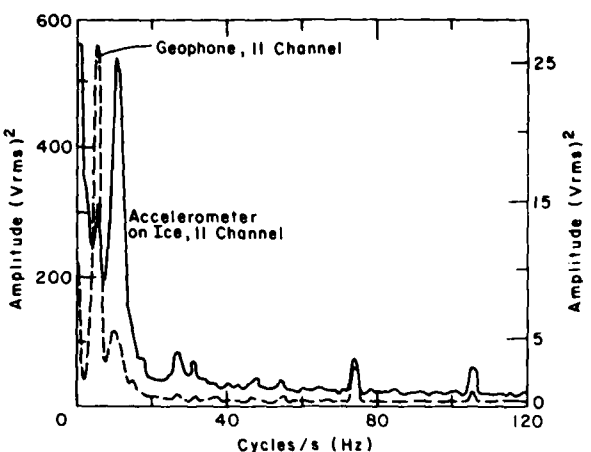


Figure 17. Auto power spectrum plots for the accelerometer on the ice and the geophone (both mounted parallel to the channel) for the Mackinaw upbound at the Gordon site. Right scale for accelerometer, left scale for geophone.

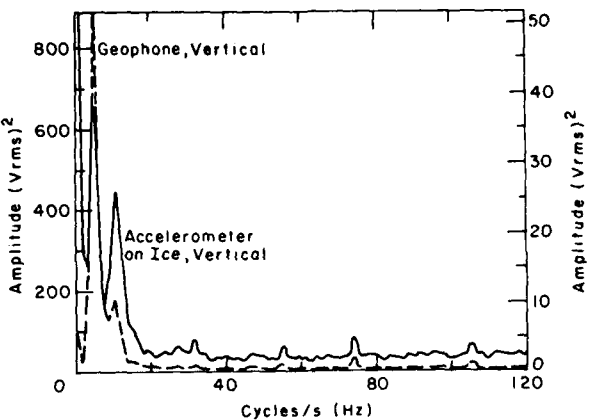


Figure 18. Auto power spectrum plots for the accelerometer on the ice and the geophone (both vertical) for the Mackinaw upbound at the Gordon site. Right scale for geophone, left scale for accelerometer.

both the geophone and accelerometer signals. Figure 17 shows the auto spectra of the y-direction accelerometer on the ice and the y-direction geophone. Figure 18 shows the auto power spectra for the vertical direction accelerometer on the ice and the vertical direction geophone.

The Roger Blough

Figure 19 is a plot of the data from the strip chart recorder for the *Roger Blough* passing the Gordon site on 22 January. The geophone signals

indicate a frequency of 8 Hz, which results from a shaft speed of 120 rpm with a four-bladed propeller. This frequency was checked with the signal analyzer. Figures 20-22 are the auto power spectrum plots of the geophones perpendicular to the channel, parallel to the channel and in the vertical direction respectively.

Figure 23 shows the magnitude of the *Roger Blough's* vibration signals on a standard vibration chart.

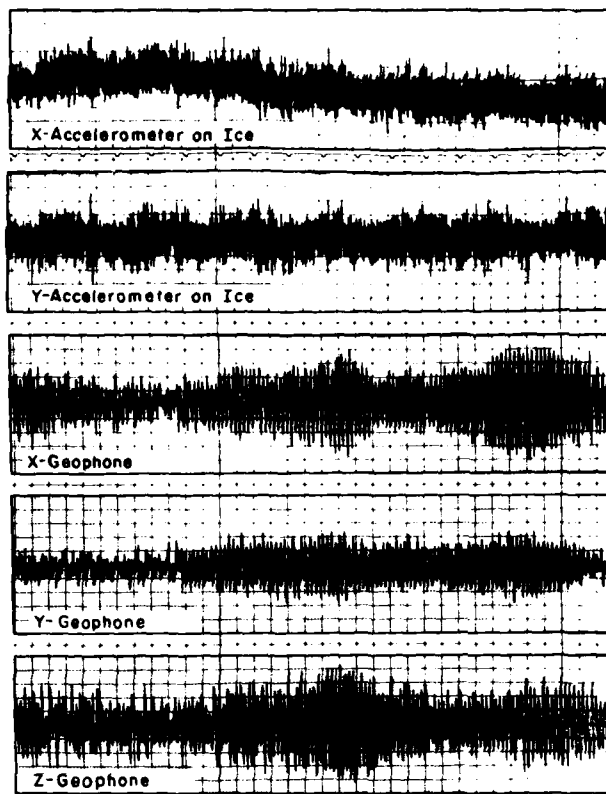


Figure 19. Signals of Roger Blough passing the Gordon site at 7.5 mph on 22 January 1979.

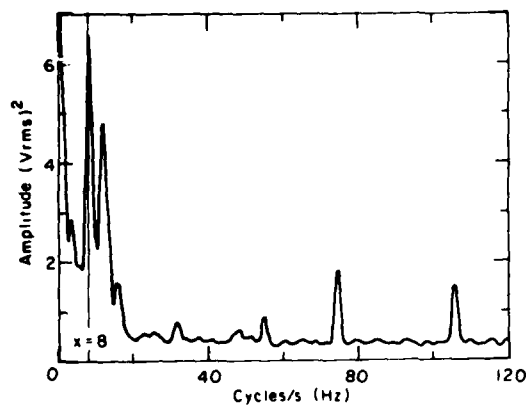


Figure 20. Auto power spectrum plot for the geophone mounted perpendicular to the channel for the Roger Blough downbound at the Gordon site.

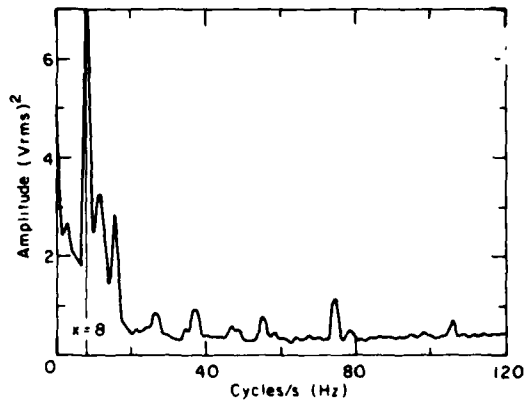


Figure 21. Auto power spectrum plot for the geophone mounted parallel to the channel for the Roger Blough downbound at the Gordon site.

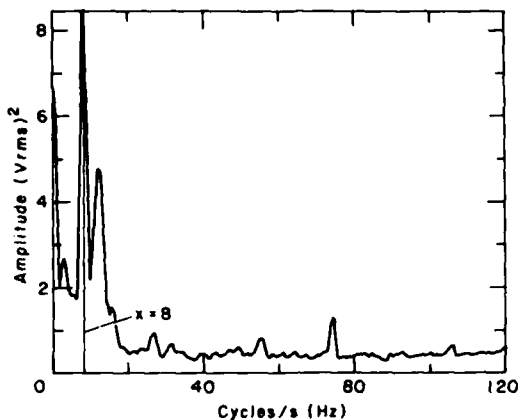


Figure 22. Auto power spectrum plot for the vertically mounted geophone for the Roger Blough downbound at the Gordon site.

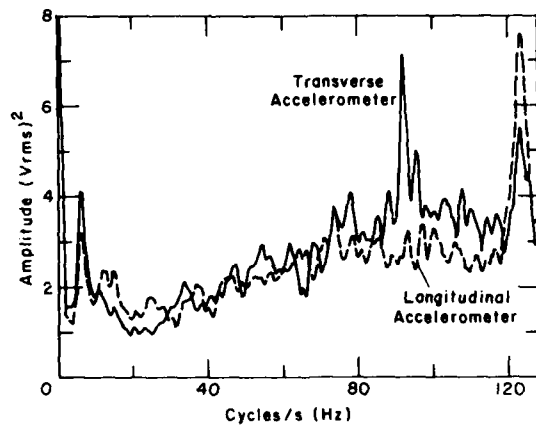


Figure 24. Auto power spectrum plots for the transverse and longitudinal direction accelerometers on the bow of the Cason J. Callaway as it passed the Gordon site downbound.

The Cason J. Callaway

On 10 February 1979 the Cason J. Callaway was boarded at the Sault Ste. Marie locks. All accelerometers were hooked up to a tape recorder and the vibration levels were measured simultaneously in the ship and on the shore as the ship passed the test sites downbound. The ship's propeller noise had a frequency of 6.7 Hz for a shaft

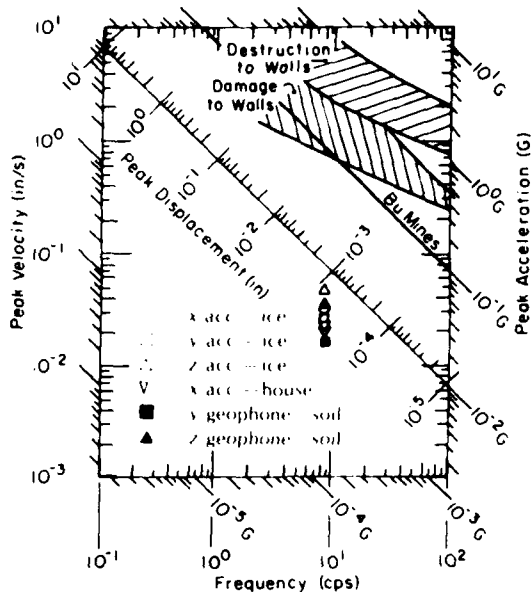


Figure 23. Magnitude of vibrations for the Roger Blough passing the Gordon site on 22 January 1979 at 7.5 mph (x is perpendicular to and y parallel to the ship channel; z is vertical).

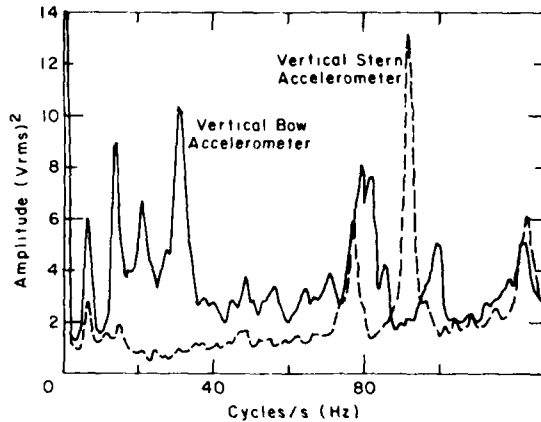


Figure 25. Auto power spectrum plots for the vertical accelerometers on the bow and stern of the Cason J. Callaway as it passed the Gordon site.

speed of 100 rpm with a four-bladed propeller. Figure 24 shows the auto power spectrum for the bow accelerometers in the transverse and longitudinal directions. The peaks at 6.5 Hz are the propeller noise since the resolution on the auto spectrum is 0.5 Hz. Figure 25 shows the auto spectrum for the accelerometers in the vertical direction, bow and stern. The peaks at 6.6 Hz are

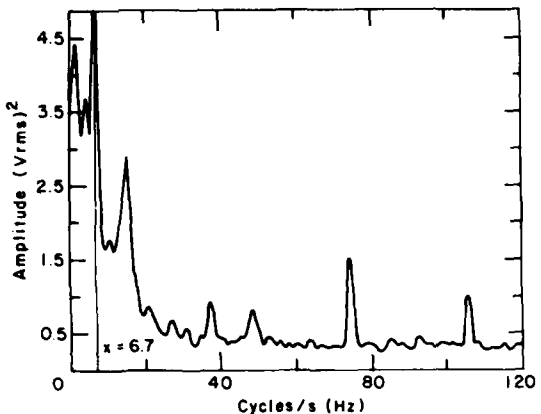


Figure 26. Auto power spectrum plot for the geophone mounted perpendicular to the channel as the Cason J. Callaway passed the Gordon site downbound.

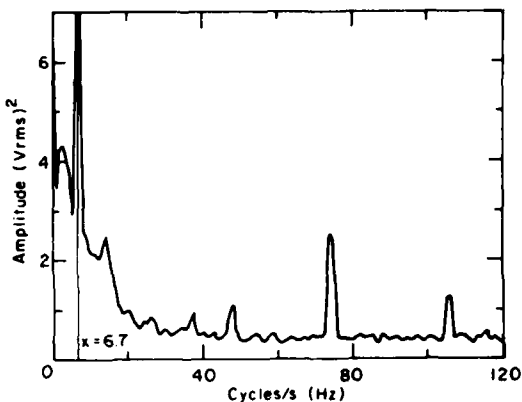


Figure 27. Auto power spectrum plot for the geophone mounted parallel to the channel as the Cason J. Callaway passed the Gordon site downbound.

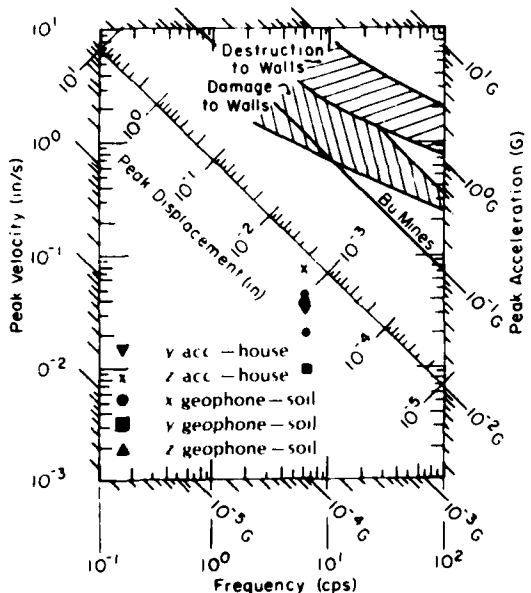


Figure 28. Magnitude of vibrations for the Cason J. Callaway passing the Doran site downbound on 10 February 1979 (x is perpendicular to and y is parallel to the ship channel; z is vertical).

the propeller noise, which is stronger for the stern than the bow, as expected. Positive identification of the propeller noise on shore is furnished by the geophone auto spectra in Figures 26 and 27. The 6.7-Hz signal was picked up by geophones as the Cason J. Callaway passed the Gordon site. This same frequency was found for the maximum vibration signals as the Callaway passed the Doran site. It should be noted that

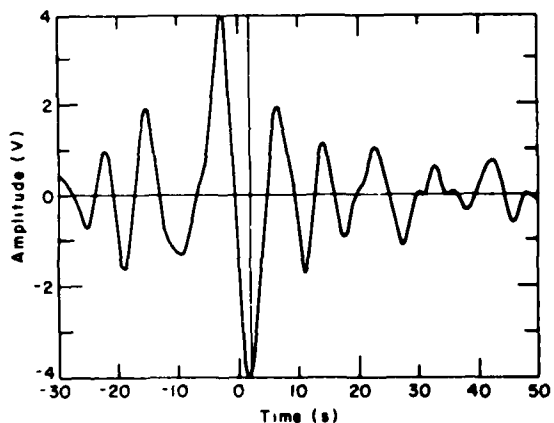


Figure 29. Time record for the accelerometer mounted in the transverse direction on the bow of the Cason J. Callaway.

none of the higher frequency components, e.g. 92 and 123 Hz, that were most dominant in the ship were detected on shore. Figure 28 shows the vibration levels for the Callaway passing the Doran site.

On 11 February 1979 the Callaway encountered some strong ice in Lake Michigan about 10 miles north of Gary, Indiana. Figure 29 shows the time record for the bow accelerometer in the

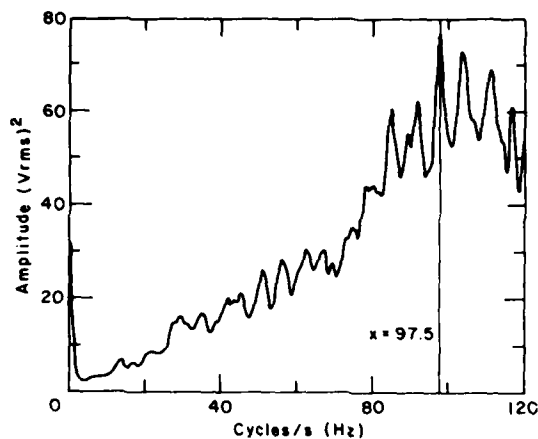


Figure 30. Auto power spectrum for the accelerometer mounted in the transverse direction on the bow of the Cason J. Callaway.

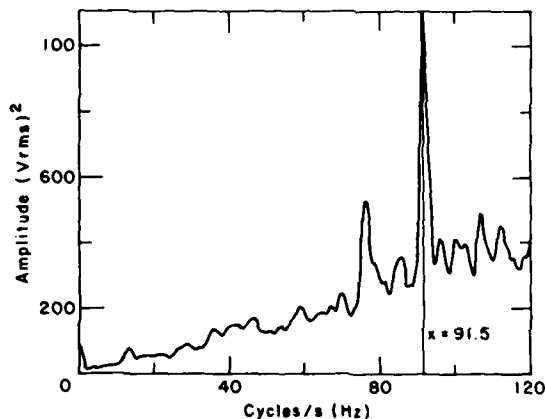


Figure 32. Auto power spectrum for the accelerometer mounted in the longitudinal direction on the bow of the Cason J. Callaway.

transverse direction. The magnitude indicates a 3.17-g level; however, the accelerometer used was linear up to 2 g so there is little confidence above that level. Figure 30 shows the dominant frequency for the transverse bow accelerometer to be 97.5 Hz. The natural frequency of the accelerometer is 104 Hz, but the internal damping ratio is 0.6 so resonance effects should be negligible. The time record for the bow accelerometer in the longitudinal direction is shown in Figure 31. A 1.42-g vibration level is indicated. Figure 32 gives the dominant frequency at 91.5 Hz for this direction. The time record for the bow accelerometer in the vertical direction is shown in Figure 33. A vibration level of 2.4 g is indicated but this exceeds the 2-g range of the

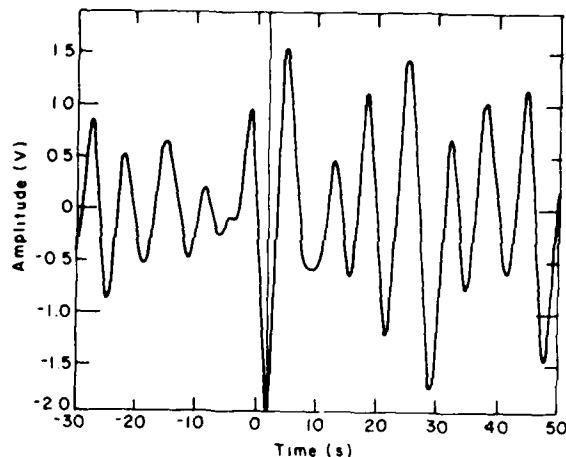


Figure 31. Time record for the accelerometer mounted in the longitudinal direction on the bow of the Cason J. Callaway

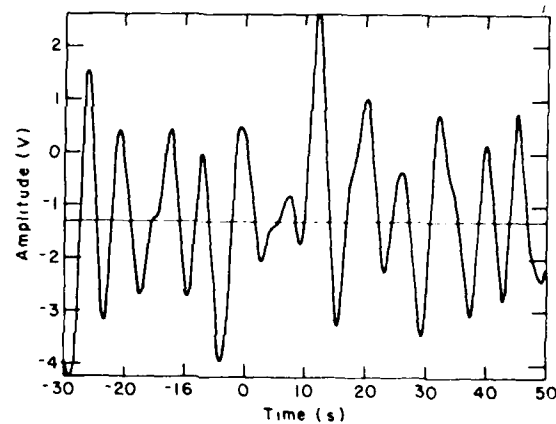


Figure 33. Time record for the accelerometer mounted in the vertical direction on the bow of the Cason J. Callaway.

accelerometer. Figure 34 shows the dominant frequency for this direction to be 91 Hz.

The three accelerometers mounted in the stern did not indicate the high frequencies or the high magnitudes that those mounted in the bow did. Figure 35 is the auto spectrum for the stern accelerometer in the transverse direction. The vibration level is about one order of magnitude lower than that found for the bow transverse accelerometer shown in Figure 30. Figure 36 is the auto spectrum for the stern longitudinal vibration. The auto spectrum for the stern vertical accelerometer is shown in Figure 37. Magnitude comparisons for vertical bow and stern accelerometers show that the bow level is about 19 times the stern level.

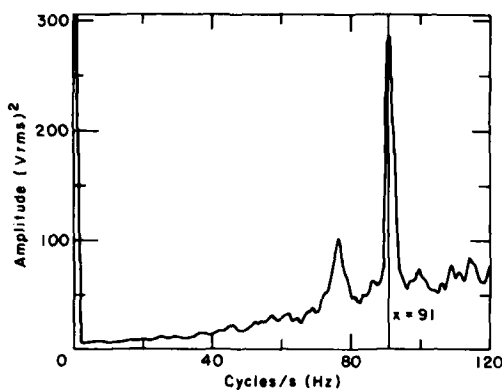


Figure 34. Auto power spectrum for the accelerometer mounted in the vertical direction on the bow of the Cason J. Callaway.

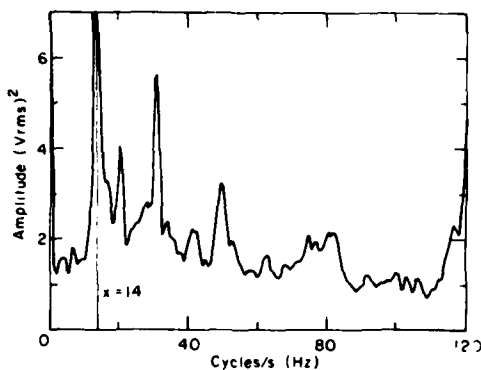


Figure 36. Auto power spectrum for the accelerometer mounted in the longitudinal direction on the stern of the Cason J. Callaway.

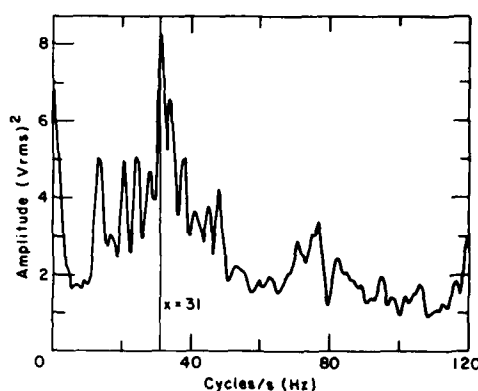


Figure 35. Auto power spectrum for the accelerometer mounted in the transverse direction on the stern of the Cason J. Callaway.

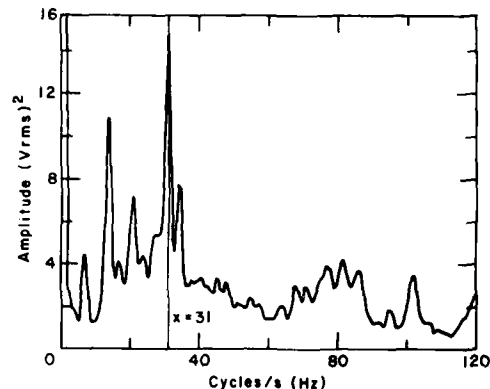


Figure 37. Auto power spectrum for the accelerometer mounted in the vertical direction on the stern of the Cason J. Callaway.

The Imperial St. Clair

In Figure 38 the *Imperial St. Clair*, a 133-m-long tanker, is shown passing the Gordon site after breakup of the ice. Figures 39 and 40 are the auto spectra of the accelerometers on the ice and house, perpendicular to the channel. The dominant frequency of 9.5 Hz in both figures corresponds to 142 rpm with a four-bladed propeller. The coherence, or measure of the degree of causality, between the two signals is shown in Figure 41. A plot of the vibration magnitudes is given in Figure 42.

Vibration levels

Figures 43-49 give the vibration magnitudes of seven ships that produced high vibration levels. The magnitudes for two ships passing the Gordon site are given in Figures 43 and 44. The

magnitudes for five ships passing the Doran site are given in Figures 45-49. All plots were made at propeller noise frequencies which were the dominant frequencies as determined from the auto spectrum graphs. For a comparison of vibration magnitudes with and without an ice cover, data were obtained for the *Philip R. Clarke* on 3 April 1979 when the channel was essentially ice-free (Fig. 50).

To answer the question of whether the vibration levels are great enough to be perceived, the maximum vibration displacements for six ship passages were plotted on a standard chart given in Harris and Crede (1975). This chart is for rotating machinery conditions and the allowable limits might tend to be higher than those acceptable for a residence. Figure 51 shows that the vibrations can be perceived. The one data point

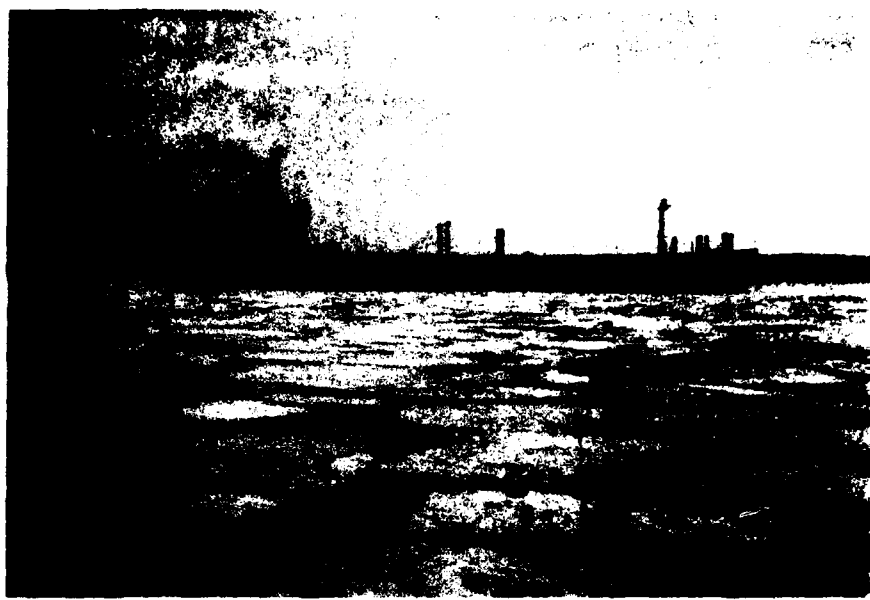


Figure 38. Imperial St. Clair passing the Doran site downbound on 21 March 1979.

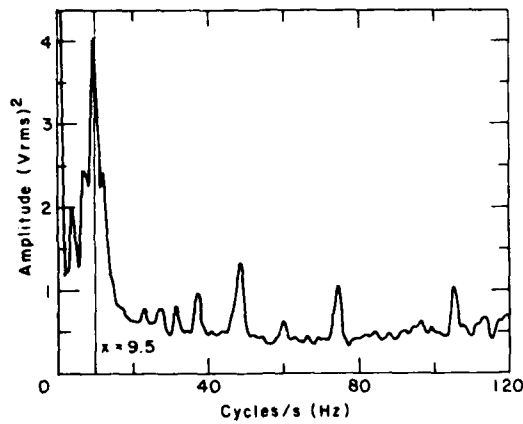


Figure 39. Auto power spectrum for the accelerometer mounted perpendicular to the channel on the ice as the Imperial St. Clair passed the Doran site.

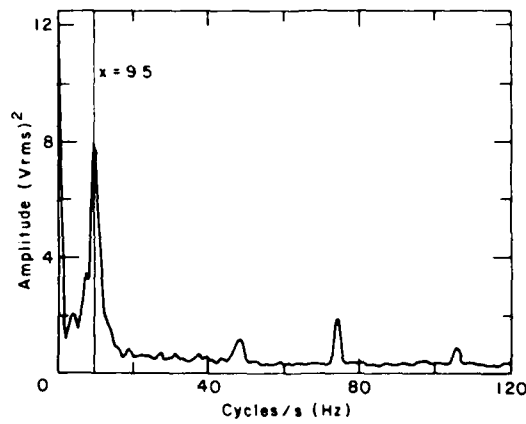


Figure 40. Auto power spectrum for the accelerometer mounted perpendicular to the channel on the house as the Imperial St. Clair passed the Doran site.

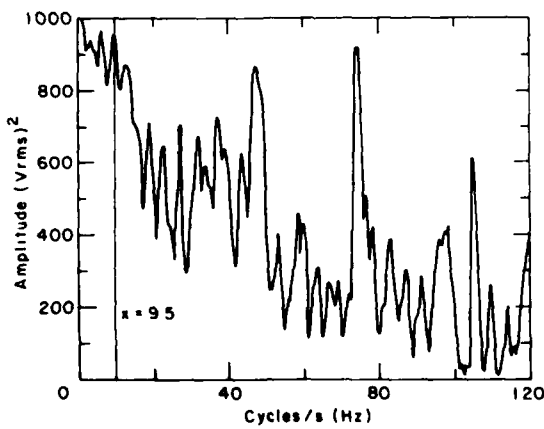


Figure 41. Coherence function for the accelerometers mounted perpendicular to the channel on the ice and house as the Imperial St. Clair passed the Doran site.

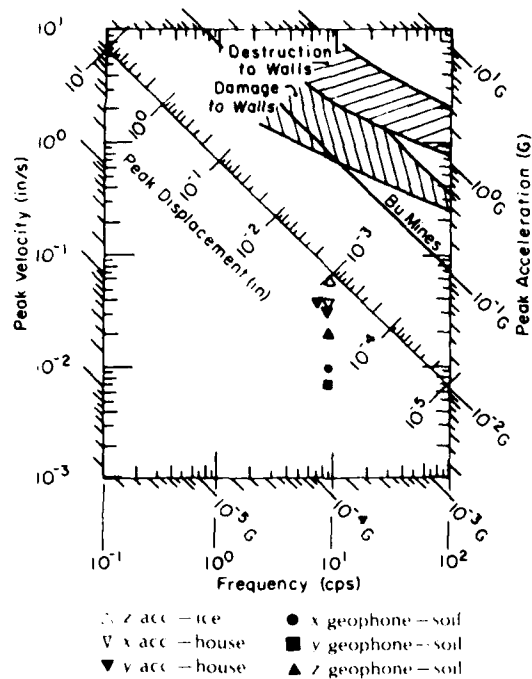


Figure 42. Magnitude of vibrations as the Imperial St. Clair passed the Doran site downbound on 8 March 1979 at 9.9 mph (x is perpendicular to and y is parallel to the ship channel; z is vertical).

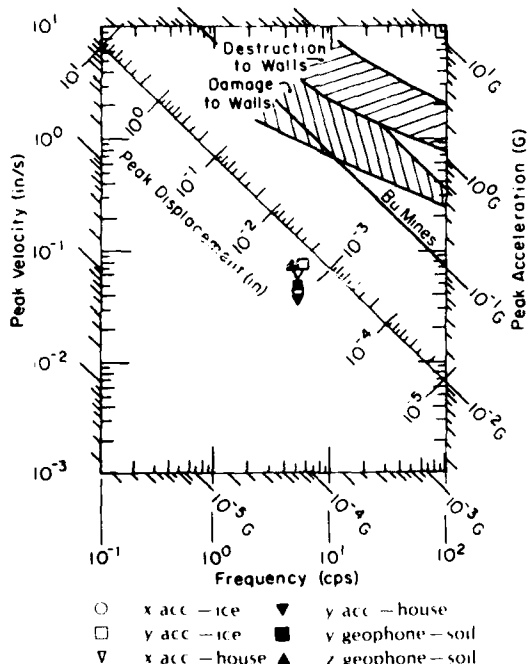


Figure 44. Magnitude of vibrations as the USCGC Mackinaw passed the Cordon site upbound on 19 February 1979 at 6.2 mph (x is perpendicular to and y is parallel to the ship channel; z is vertical).

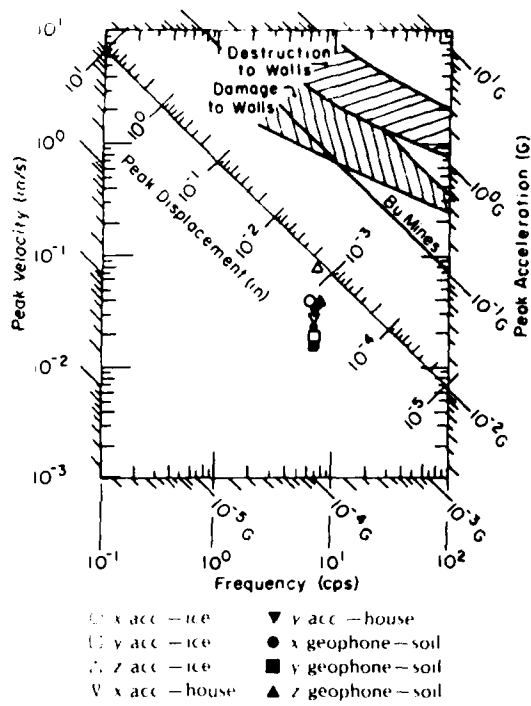


Figure 43. Magnitude of vibrations as the George Stinson passed the Cordon site downbound on 23 January 1979 at 7.4 mph (x is perpendicular to and y is parallel to the ship channel; z is vertical).

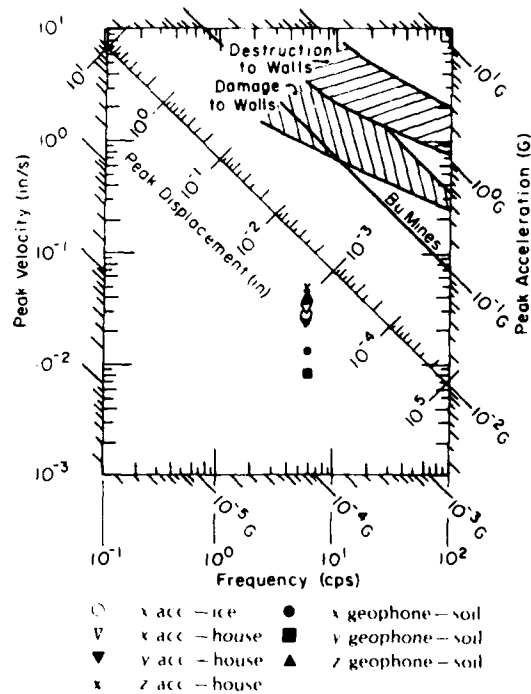


Figure 45. Magnitude of vibrations as the USCGC Mackinaw passed the Doran site upbound on 16 February 1979 at 8.5 mph (x is perpendicular to and y is parallel to the ship channel; z is vertical).

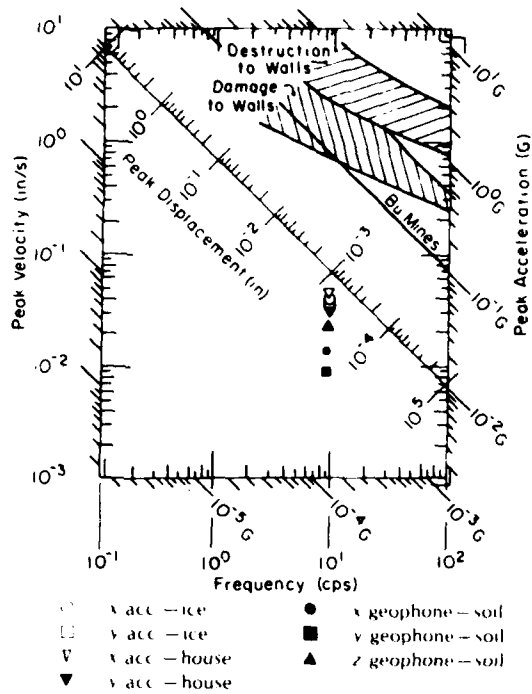


Figure 46. Magnitude of vibrations as the Roger Blough passed the Doran site upbound on 18 March 1979 at 7.4 mph (x is perpendicular to and y is parallel to the ship channel; z is vertical).

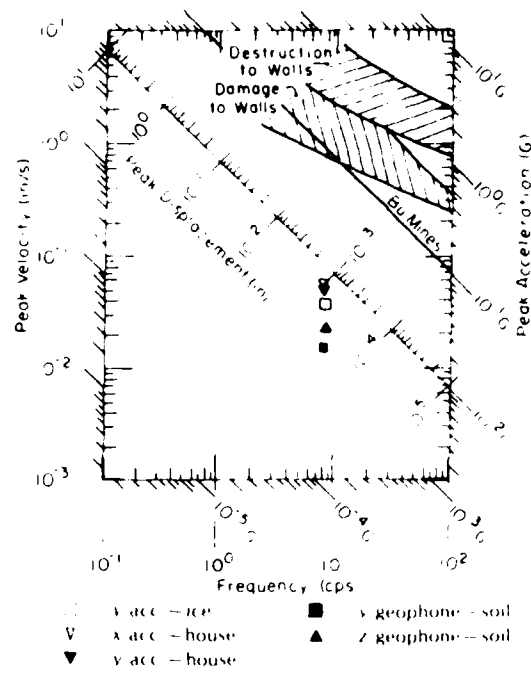


Figure 47. Magnitude of vibrations as the Roger Blough passed the Doran site upbound on 24 February 1979 at 6.8 mph (x is perpendicular to and y is parallel to the ship channel, z is vertical).

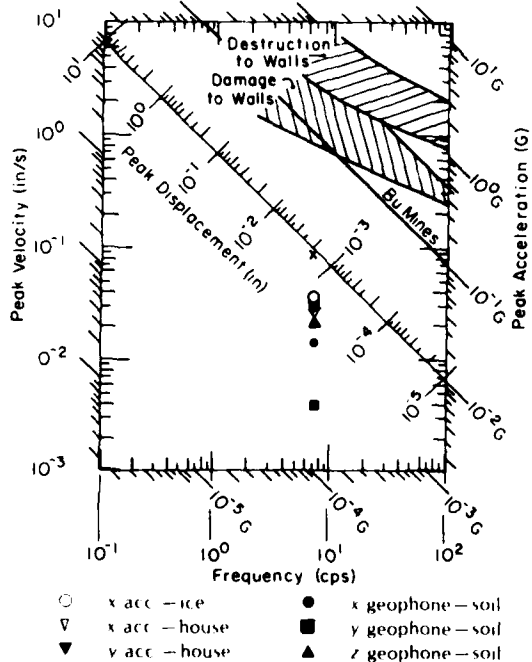


Figure 48. Magnitude of vibrations as the Philip Clarke passed the Doran site downbound on 10 February 1979 (x is perpendicular to and y is parallel to the ship channel; z is vertical).

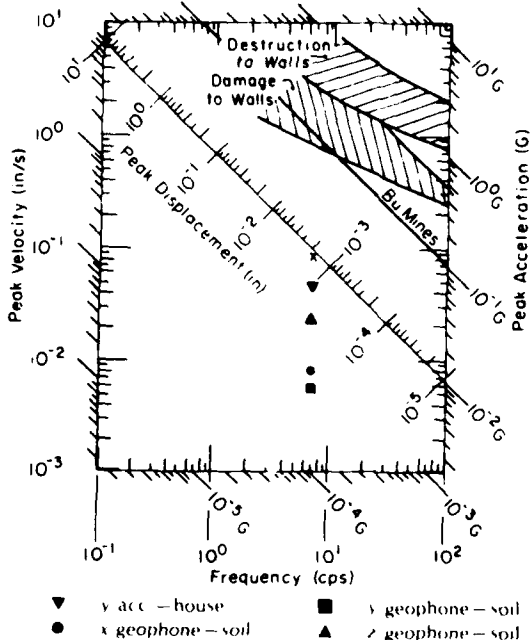


Figure 49. Magnitude of vibrations as the Philip Clarke passed the Doran site downbound on 21 March 1979 at 11.5 mph (x is perpendicular to and y is parallel to the ship channel; z is vertical).

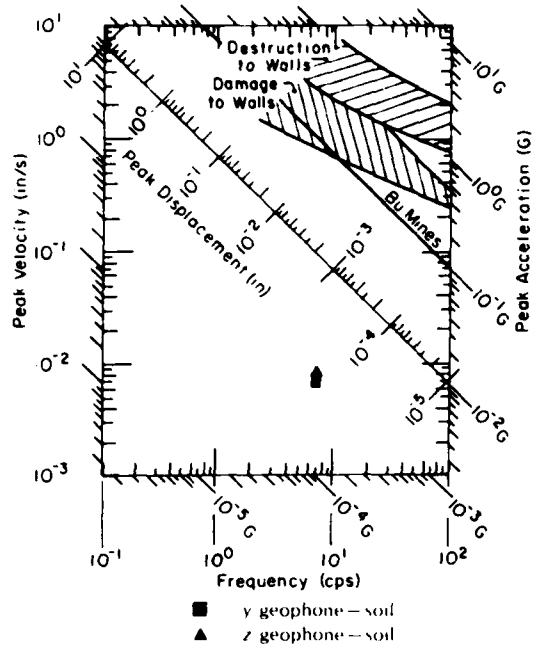


Figure 50. Magnitude of vibrations as the Philip Clarke passed the Cordon site downbound on 3 April 1979 at 9.3 mph in open water.

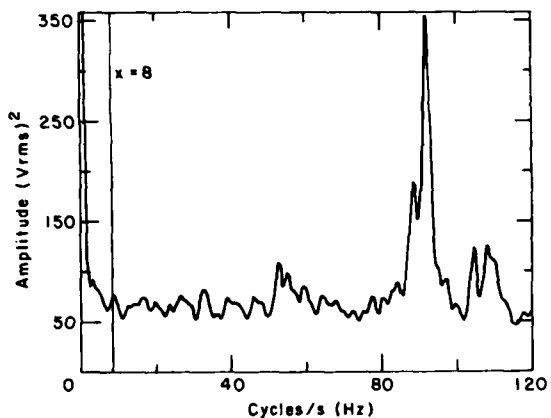


Figure 52. Auto power spectrum for the hydrophone as the Roger Blough passed the Doran site.

for the open water condition is barely above the threshold of perception.

The hydrophones were able to pick up the propeller noise (Fig. 52) as well as frequencies that are related to ice crushing against the bow of the ship. Figure 53 is a time average plot. The maximum signal in Figure 53 represents a pressure increase of 0.103 kPa (0.015 psi).

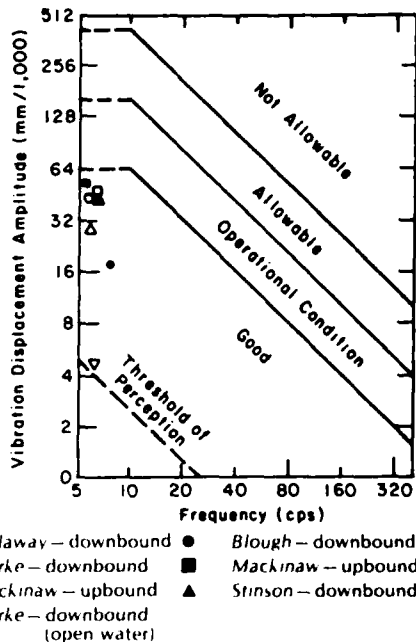


Figure 51. Levels of vibration for seven ships passing the test sites (white symbols represent the Doran site, dark symbols the Cordon site).

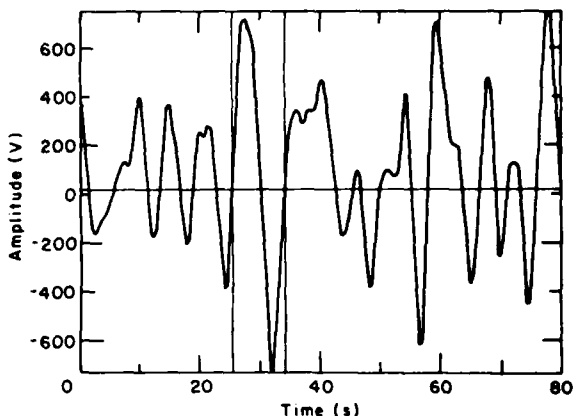


Figure 53. Time record for the hydrophone as the Roger Blough passed the Cordon site.

DISCUSSION

Frequency content

The test results show that vibrations caused by ships can be detected. Vibration frequencies caused by propeller noise can be seen on the strip chart recorder plots: Figure 14 for the USCCC Mackinaw and Figure 19 for the Roger

Blough These frequencies were verified with a signal analyzer. This cross-check method was done for each ship mentioned in this report. Ship propeller frequencies were detected by transducers on the ice, in the soil and on the houses. Figures 39 and 40 show that the same dominant propeller noise frequencies were detected by the accelerometers on the ice and house for the *Imperial St. Clair*. Figure 41 shows a high coherence or measure of causality between these two signals.

It is possible that a source other than a ship's passing could cause vibrations. Dr. David Willis (pers. comm.) determined that vehicle traffic on a nearby road caused vibrations in the same frequency range (5-10 Hz) as the ships. However, the magnitude of the vibrations caused by the vehicle traffic was about 15% of that recorded for the ships, and the transducers in the house were located about 150 m from the road at both sites.

Ship vibration problems are discussed by Noonan and Feldman (1978). They list the vibration problem areas on a ship as vibration of hull girder, major substructures, local structural elements, shipboard equipment and main propulsion system. Stiansen (1978) points out that propeller-induced vibratory forces are the most serious of all periodic forces. These forces may be transmitted to the hull directly by shaft bearings or indirectly by the unsteady water pressure field acting on the hull near the stern. Sheet cavitation on the propeller blades can be the most severe source of ship vibrations. Cavitation problems can be attenuated with highly skewed and variable pitch propellers. However, these ship vibration problems are not the same as those associated with icebreaking or a ship going through brash ice.

Dean (pers. comm.) has determined the frazil and brash ice thickness in the study area. He used airborne radar system profiling and ground truth measurements to determine the accumulated ice thickness on the St. Marys River between Frechette Point and Six Mile Point on 8 March 1978. The accumulated frazil and brash ice thickness measured 4 to 5 m. The porosity of the frazil portion of the mass was determined to be 0.6 to 0.4. The brash and frazil ice thickness was not determined in 1979 and we assumed that it was somewhat less than that reported by Dean for 1978.

Figure 24 shows that the propeller-blade-induced vibration is detected by the bow accelerometers on the *Cason J. Callaway*. It also shows

that there are some dominant frequencies at 92.5 Hz and 123.5 Hz that are associated with icebreaking and with the ship passing through the brash ice which filled the channel. These high frequencies were not the dominant frequencies detected by transducers on the ice and shore. This is probably due to higher attenuation of high frequency signals. Figure 25 shows the propeller noise to be stronger in the stern than in the bow, as expected. It also shows some dominant peaks at 13.8, 21.0 and 31.0 Hz that are probably due to rotating machinery in the stern. For example, $20 \text{ Hz} \times 60 = 1200 \text{ rpm}$, which is the speed of the a.c. and d.c. generators on board the *Callaway*. The dominant 92.0-Hz frequency is probably associated with the bow colliding with the brash ice in the channel.

The strong ice encountered by the *Callaway* on 11 February, 10 miles north of Gary, Indiana, resulted in crushing and breaking of ice since there was no open track. Figure 30 indicates that the highest energy is at a frequency of 97.5 Hz as detected by the transverse bow accelerometer. Figure 32 shows a frequency of 91.5 Hz was detected by the longitudinal bow accelerometer and Figure 34 gives a frequency of 91 Hz detected by the vertical bow accelerometer. An interesting feature is that the energy of transverse vibrations at the bow is spread from 80 to 150 Hz, with longitudinal and vertical vibrations having only a narrow peak at 91 Hz. This indicates that the bow vibrations are local and must be related to ice crushing and failing against the bow.

Ormondroyd (1950) investigated stresses and natural frequencies on the USCGC *Mackinaw*. A vibration generator was mounted on the centerline of the upper deck to excite the natural modes in the vertical plane. This was done for both open deep water (24 m under the hull) and open shallow water (0.6 m under the hull). For deep water the first mode (two nodes) had a frequency of 3.5 Hz and the second mode (three nodes) had a frequency of 6.2 Hz. Rigid body motion of the ship was negligible in comparison to resonant vibration amplitudes. Figures 54 and 55 show that the first and second modes were detected by the vertical direction accelerometer on the ice and the vertical geophone in the soil.

Magnitude

All of the tapes were played out on a Brush strip chart recorder in order to identify the ships that caused the largest vibrations. After these ships were identified, their vibration records

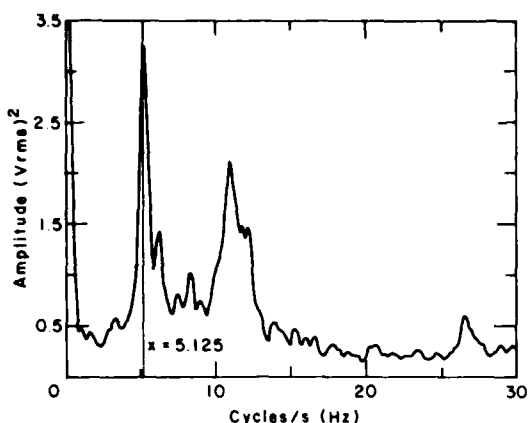


Figure 54. Auto power spectrum for the accelerometer mounted on the ice in the vertical direction as the USCGC Mackinaw passed the Gordon site upbound.

were examined in detail. Maximum vibration signals were found for each transducer and the results were plotted on a standard vibration chart taken from Harris and Crede (1975). These vibration signals were plotted at the dominant frequency as seen on the strip chart record and verified with an auto power spectrum analysis.

Ground motion studies generally assume that a particle velocity of 25.4 mm/s will cause damage to a building. However, at present a reduction in this particle velocity level is being considered for design codes. Vibration magnitudes for the ships which caused the highest vibrations are given in Figures 15, 23, 28 and 42-50. Most of the signals ranged from 0.18 mm/s to 2.3 mm/s. These levels are about an order of magnitude lower than levels required to cause damage to the walls of a building.

Residents along the channel felt that the vibrations were lower in 1979 than in other years. There are at least two reasons why the levels were lower. First, there were no significant ice jams in 1979 so that ships, especially the Mackinaw, did not have to back up and ram the ice, the situation which residents felt caused the most serious vibrations in previous years. Residents feel that the boom placed at the Little Rapids Cut has reduced the occurrence of and potential for ice jams. Second, the snow depth on the ground for most of the winter was about 0.8 m, which prevented the ground from freezing. The ground was not frozen in January when the geophones were buried. This unfrozen soil could reduce the vibration levels by not providing a continuous frozen layer from shore to house

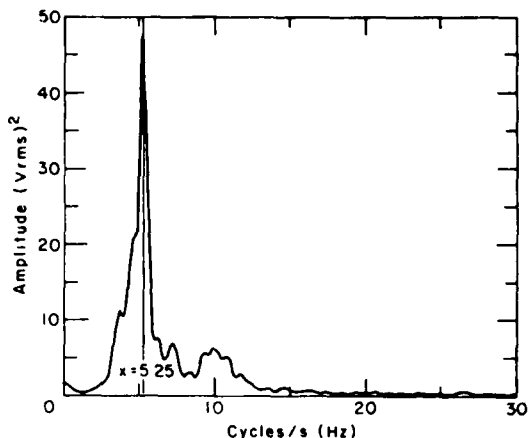


Figure 55. Auto power spectrum for the geophone mounted in the vertical direction as the USCGC Mackinaw passed the Gordon site upbound.

Unfrozen soil, with its lower modulus, causes greater damping of vibration signals.

All of the magnitude records show that the vertical direction geophone had the largest velocity of the three geophones. In some cases, as in Figures 15, 23, 42 and 43, vertical particle motion was the largest motion detected on the ice. Data from the accelerometers mounted on the Callaway show that vibration levels on the bow were more than an order of magnitude higher than those on the stern. This is due to high local acceleration on the bow associated with ice-breaking.

It is difficult to make exact comparisons of vibration levels for ship traffic with and without an ice cover because of different ship speeds and subsequent energy input to the water. However, some rough estimates have been made (Table 1). The vertical direction geophone signal was used for the comparison since it always indicated the largest soil particle motion.

The first comparison in Table 1 is the most reasonable, since it involves the same ship going the same direction, downbound, for ice and no-ice conditions. The ship speed is higher for the no-ice condition but the unknown shaft speed and energy input could have been the same or less for the no-ice condition. In the second comparison, a broken ice condition as shown in Figure 38 is used and a lower ratio is found, as expected. In the third comparison two similar ships with quite different speeds are used to obtain a high ratio. From one year's data it appears that the vibration level with an ice cover is about four to five times the vibration level without an ice cover.

Table 1. Comparison of vibrations with and without an ice cover.

Condition	Ship	Power MW (hp)	Date <1979>	Speed km hr (mph)	z Geophone mm s	Ratio
Ice	Clarke (Dn)	5.2 (7,000)	10 Feb	13.8 (8.6)	0.889	
No ice	Clarke (Dm)	5.2 (7,000)	3 Apr	15.0 (9.34)	0.216	4.1
Broken ice	Clarke (Dm)	5.2 (7,000)	21 Mar	18.5 (11.32)	0.610	
No ice	Clarke (Dm)	5.2 (7,000)	3 Apr	15.0 (9.34)	0.216	
Ice	Callaway (Dm)	5.2 (7,000)	10 Feb	13.8 (8.6)	1.054	
No ice	Algolake (Up)	6.0 (8,400)	7 Apr	8.4 (5.24)	0.127	8.3

Table 2. Comparison of vibrations with solid ice and broken ice.

Condition	Date <1979>	Ship	Speed km hr (mph)	z Geophone mm s	Ratio
Solid	27 Jan	Anderson (Up)	N/A	0.295	
Broken	21 Mar	Anderson (Dm)	19.1 (11.86)	0.417	
Solid	24 Feb	Blough (Up)	10.9 (6.8)	0.584	
Broken	18 Mar	Blough (Up)	11.8 (7.35)	0.686	0.85
Solid	10 Feb	Callaway (Dm)	13.8 (8.6)	0.295	
Broken	18 Mar	Callaway (Up)	15.6 (9.68)	0.295	1.0
Solid	16 Feb	Clarke (Dn)	13.4 (8.3)	0.503	
Broken	21 Mar	Clarke (Dm)	18.5 (11.5)	0.521	0.96
Solid	8 Mar	Imperial St. Clair (Dn)	15.9 (9.9)	0.500	
Broken	21 Mar	Imperial St. Clair (Dn)	12.6 (7.8)	0.429	1.17
Solid	11 Mar	USCGC Katmai Bay (Dn)	23.3 (14.5)	0.236	
Broken	21 Mar	USCGC Katmai Bay (Dn)	22.5 (14.0)	0.208	1.13

**Figure 56. Accelerometers mounted on the ice, and shoreline crack.**

When the ice is broken up the ratio is about two to three times that of a no-ice condition. This suggests that the energy transmission is not all through the ice but that some is through the water, with the ice, solid or broken, acting as a waveguide.

To identify the mode of vibration energy transmission, a comparison was made between the solid ice and broken ice conditions. These two conditions are shown in Figures 5 and 7 respectively. The solid ice has many cracks in it, e.g. the shoreline crack shown in Figure 56. These cracks are dry, however, and the ice sheet is continuous. In contrast, the broken ice condition is a discontinuous ice sheet (Fig. 38). Table 2 gives vibration levels for six ships under the two conditions. Again, the vertical direction geophone signal was used for the comparison, except for the Callaway, where the signal from the geophone parallel to the channel was used.

The results shown in Table 2 indicate that the vibration levels, as detected in the soil, are about the same for a solid ice sheet and for a broken-up ice sheet. Rigorous comparisons cannot be made because of different ship speeds and unknown power expenditure. Shaft rpm is about the same for the comparisons but ship speed would generally increase in broken ice with the same rpm.

Mode of transmission

The data collected in this study enabled the propeller-excited vibrations to be clearly identified by the geophones buried in the soil on shore. The energy path from the propeller to the geophones could be through three modes: 1) in the water, 2) in the soil, and 3) in the ice. Each of these modes will be discussed, with the knowledge that the vibration levels with an ice cover are about four times the levels without an ice cover, and that there is not much difference between the vibration levels with a solid ice sheet and a

broken ice sheet. Also, the discussion will focus on the fact that the vertical motion was the largest, as measured by the buried geophones. Figure 57 shows the three modes and their paths.

Energy is transmitted through the water by a compressional wave or *P* wave. In his discussion of the transmission of seismic waves from a liquid to a solid, White (1965) reports that the reflection coefficient is near unity for incident angles greater than 60° from the normal. This means that *P* waves in the water, successively reflected between the bed and the ice, could propagate to shore with little attenuation and no change in waveform. This reflection of *P* waves will also occur without an ice cover. To account for the higher energy with an ice cover, the explanation may lie with the *P* wave interaction with the shore-fast ice. The incident *P* wave could cause a refracted *P* wave and a refracted shear or *S* wave in the ice above and in the soil on the bottom. The wave energy is thereby being focused or absorbed in a way similar to the high energy absorption by wedged surfaces in an anechoic room. Without an ice cover the incident *P* wave causes refracted waves only in the soil on the bottom. The refracted shear waves in the ice and in the bottom soil could combine to produce a vertical shear or *SV* wave to account for the large vertical vibration signals detected by the geophones.

There will be energy transmission through the soil with or without an ice cover. The incident *P* wave will cause refracted *P* and *S* waves and Rayleigh waves in the bed. These will propagate to shore. Reflected *P* waves from underlying bedrock and refracted *P* waves from denser layers, which could cause large vertical component vibrations, are not considered because they will be unaffected by the presence of an ice cover. As the *S* waves and Rayleigh waves propagate towards shore their energy could be amplified by the interaction with incident *P* waves from the

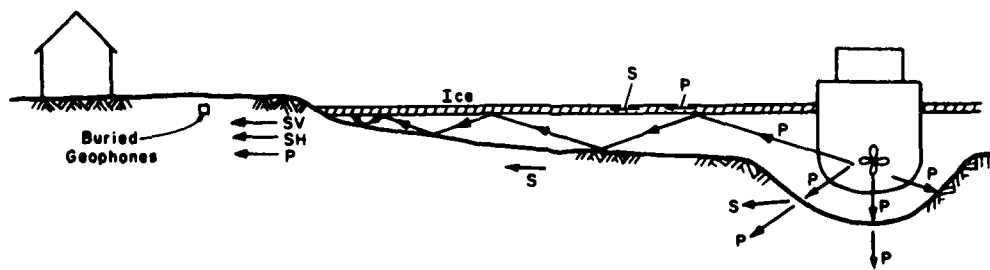


Figure 57. Seismic wave paths.

water. This resonant coupling could be greater with an ice cover than without, especially very close to shore. These amplified SV waves could then account for the large vertical component of vibration detected on shore.

Incident P waves from the water can cause refracted P and S waves in an ice cover. These S waves can propagate towards shore and cause the large vertical vibration signals that we obtained. However, the results in Table 2 indicate that there is not much difference in vibration levels between solid ice and broken ice. The broken-up ice pieces would all have to be in contact for the S waves to be transmitted to shore. The P waves could be transmitted to shore whether the ice pieces were in contact or not and could possibly generate S waves where the shore-fast ice contacts the shore.

Since all three modes are possible, a definitive answer to the question of wave energy transmission must be deferred until additional data are obtained. However, based on only one year's data, the dominant modes of energy transmission appear to be 1) a P wave through the water, with the ice acting as a waveguide to focus the energy as it approaches the shore, and 2) resonant coupling between P waves in the water and S waves or Rayleigh waves in the bed. Further study should include the use of additional instrumentation to delineate the contribution from each mode.

Opening the channel

During the winter navigation season ice-breaking on the St. Marys River is vital to ship passage. On 10 February 1979, the USCGC *Katmai Bay*, with a 12.1-m beam, passed the test sites in the morning. Eight hours later the *Callaway* passed the sites downbound as discussed in the test results section. One-half hour later a sister ship, the *Philip R. Clarke*, followed the *Callaway* downbound. The *Callaway* and *Clarke* both have a 23-m beam and were both traveling at the same velocity of 13.8 km/hr (8.6 mph). The vibrations on the *Clarke* were only 45 to 67% of those measured on the *Callaway*. This verifies the importance of the icebreaking process in producing vibrations on shore. The high vibration levels caused by icebreaking are partly due to the icebreaking itself and partly due to the higher power demand.

Flexural waves

One phenomenon which is evident in Figures 14 and 19 is the waves picked up by the acceler-

ometers mounted on the ice. The accelerometers used were sensitive to tilt in the vertical plane, so any tilt in the ice will be detected by them. Tilt of the accelerometer perpendicular to the channel is evident in both figures and represents a flexural wave in the ice as a water wave is progressing toward shore. To a lesser degree, tilt of the accelerometer parallel to the channel is shown in Figure 14. The accelerometers used had a frequency range starting from zero so that the quasi-static tilt component could be determined. The magnitude of tilt for the accelerometer perpendicular to the channel in Figure 14 is 0.86°. The period is about 18 s. The velocity of flexural waves for ice in shallow water is

$$V = (gh)^{1/2} \quad (1)$$

where h is the water depth. For the Gordon site, $V = 3.5 \text{ m/s}$ (11.35 ft/s) so the wavelength is

$$\lambda = Vf = 62.3 \text{ m} (204 \text{ ft}) \quad (2)$$

In Figure 19 the magnitude of tilt is 0.7° for the accelerometer perpendicular to the channel. The period and wavelength are the same as above.

The presence of tilt shown by the accelerometer parallel to the channel, concurrent with tilt shown by the accelerometer perpendicular to the channel, indicates a flexural wave at some angle which is not normal to the shore. This is reasonable if the flexural wave is caused by the bow wave of the ship. To obtain a rough estimate of the rise and fall of the ice sheet during the passage of a flexural wave, use

$$\sin 0.86^\circ = (z\pi)/(6.23/2) \quad (3)$$

Solving for z gives 0.15 m (0.5 ft) for the wave in Figure 14. This compares well with measurements made by Gleason (pers. comm.).

Peters (1950) investigated the effect of a floating mat on water waves. This mat could be considered a field of broken ice. He formulated the problem in terms of a velocity potential $\Phi(x, y, z, t)$ with a general solution of

$$\Phi = \phi_1(x, y, t) \cos \omega t + \phi_2(x, y, t) \sin \omega t \quad (4)$$

where ω is the circular frequency and t is time.

If $\eta = \eta(x, 0, z, t)$ is the displacement of the water surface, he found that ϕ_1 and ϕ_2 are harmonic functions which must satisfy

$$p + \rho g \eta - \rho(d\Phi/dt) = 0 \quad (5)$$

$$(d\Phi/dy) + (d\eta/dt) = 0 \quad (6)$$

where eq 5 is from Bernoulli's law where the non-linear terms have been neglected in this first order approximation. Here p is the pressure at the surface, ρ is the water density, and g is the acceleration due to gravity. Now, it is assumed that gravity and the pressure of the water under the mat are the only forces acting. If ρ_i is the ice density then buoyancy per unit area is

$$\rho = \rho_i (d^2\eta/dt^2) \quad (7)$$

and Peters finds the displacement of the matted surface to be

$$\eta = -(\omega/g)[(eg)/(eg - \rho_i \omega^2)]$$
$$[\phi_1(x,0) \sin \omega t - \phi_2(x,0) \cos \omega t] \quad (8)$$

Peters points out that the effect of the broken ice depends upon the sign of $C = eg/\rho_i \omega^2 - eg$. If $C < 0$, waves pass into the broken ice with an altered wavelength and amplitude. If $C = 0$, the situation is one where waves are approaching a dock. If $C > 0$, the disturbance in the free surface is not propagated to any great distance inside the broken ice but attenuates with $1/d$ where d is the distance inside the broken ice.

If the above criteria are applied to the results of this study, the flexural waves previously discussed will have $C = -1.125$. This means that a gravity wave disturbance would pass into the broken ice pieces. If we consider a surface wave generated by a propeller with a blade frequency of 8 Hz, we obtain $C = 0.00043$. This means that the surface wave disturbance would be greatly attenuated by the broken ice pieces. A portion of the original wave energy, however, may be transmitted under the ice in the form of a *P* wave.

An observation by Wuebben (1978) of the ice off Frechette Point (300 m upstream from the Gordon site) indicates the energy associated with water waves under an ice cover. He placed an ice chisel in a nearshore ice crack and observed a 0.9 m water wave spurt through the crack as the *Philip R. Clarke* passed at about 18.4 km/h (11.4 mph). Wuebben also discusses the bow wave generated by a moving ship. As a ship approaches the critical wave velocity, which for a 1.31-m (4-ft) water depth is about 18.4 km/hr (11.4 mph), the wave-making energy becomes

concentrated in a single leading wave. He also noticed that the ice chisel vibrated furiously as the ship passed.

Duration and occurrence of maximum vibrations

The duration of strong vibration signals was determined from the strip chart records. Figures 14 and 19 show typical duration signals for the ships passing a test site where a strong signal lasted for about 10-20 s. This is comparable to signal durations found on some earthquake accelerograms (Clough and Penzien 1975). Since the time required to pass a particular site was about 60 s, the duration of vibration could potentially also be about 60 s.

The maximum vibrations measured were on the bow of the *Callaway* in the transverse direction when it was crushing ice. The level was over 2 g. A dominant frequency associated with that occurrence was 97.5 Hz (Fig. 30). The vibration in the longitudinal direction on the bow of the *Callaway* was 1.42 g and the dominant frequency was 91.5 Hz (Fig. 31). In Figure 52, the signal from the hydrophone had a maximum at 92 Hz as the *Blough* passed the Doran site. These results indicate that maximum vibrations on board ship occur when ships crush through ice, and that frequencies from 80-150 Hz are associated with that crushing.

Effect of weather

Climatological data for Sault Ste. Marie, Michigan, furnished by NOAA, were examined to determine the variation of the weather in 1978 and 1979 from the norm. Data for the years 1971-79 were of particular interest since these were the 8 years of the demonstration program. The 1.3-m snowfall in December 1978 was a record high. This is 67% above the average for the 8 years of the program and 90% above average for the 40 years of record. The average temperature for December 1978 was -7.8°C which is 4% below average for the 8 years of the program and 12.7% below average for the 40 years of record. The record snowfall in December 1978 did not allow the soil to freeze.

We investigated the effect that weather conditions might have on the level of vibrations. Figure 58 shows the average daily temperature for Sault Ste. Marie, Michigan from 1 January to 8 April 1979. The data for this figure were obtained from NOAA (1979). The first data were collected at the Gordon site on 18 January and at the Doran site on 7 February. We postulated

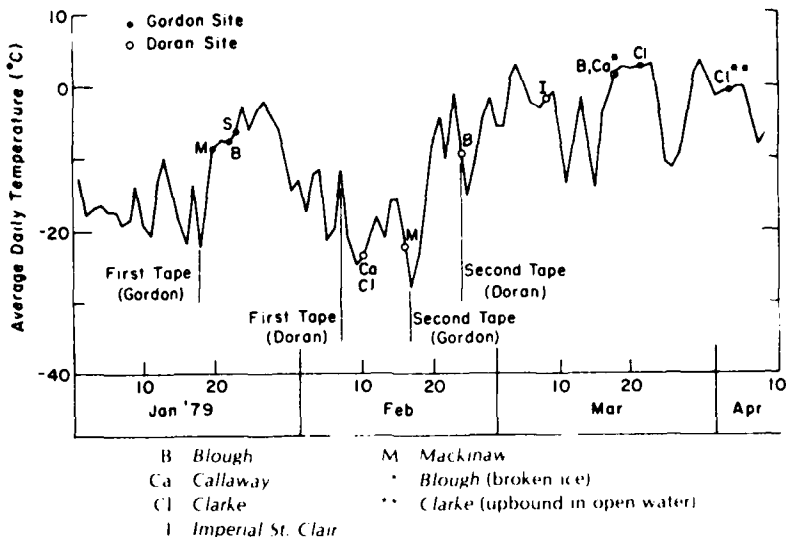


Figure 58. Average daily temperature for 1 January through 10 April 1979, Sault Ste. Marie, Michigan.

that cold, high modulus, low damping ice could transmit high vibration levels. In Figure 58, the highest vibration levels found are associated with the first six ships in chronological order. The passage of ships did not always concur with low temperatures. The first three ships, *Mackinaw*, *Blough*, and *Stinson*, were recorded after a cold period, 16-18 January, and at the beginning of a warming cycle. The next three ships, *Callaway*, *Clarke* and *Mackinaw*, were recorded at the Doran site during a definite cold period. After 20 February the weather remained comparatively warm and the vibration levels tended to be lower. However, many other variables are involved in the vibration levels produced, such as ship speed, energy expended, ship size and soil conditions. It appears that there is no definite conclusion to be reached on the weather effect from the data of 1979. The uncoupling effect of the unfrozen soil tended to dampen out any weather effect.

The vibration levels from the Gordon and Doran sites were about the same. This indicates that the shoreline protection used, i.e. rock and timber for the Gordon site and driven sheet piling for the Doran site, does not have a significant effect. Again, however, the unfrozen soil could have attenuated this effect.

There is some evidence, as indicated on the strip chart records, that other site-specific conditions might have an effect. At the Gordon site, strong vibration levels were seen when the ship was upstream of the site, both for downbound

and upbound ships. This indicates that there may be certain soil or river bed conditions favorable for energy transmission. A river bed seismic survey including core sampling must be conducted to verify this evidence.

An attempt to lump together all of the factors contributing to onshore vibration cannot be made from one year's data. However, the data suggest the dependence of the vibration on the velocity of the ship, the energy expended by the ship, the cross-sectional area of the ship, and factors which identify the condition of the ice, soil and site.

CONCLUSIONS AND RECOMMENDATIONS

The first two objectives of this study were achieved. The ships were identified as a source of vibrations. The magnitude of the vibrations was measured and the highest levels were found to be 2.3 mm/s as measured by the buried geophones, or about one order of magnitude lower than levels which could cause damage to walls. The highest levels were in the vertical direction on the ice, in the soil and on the buildings. The dominant frequencies were identified as propeller noise. Transducers on board ship indicated that frequencies of around 80-150 Hz were associated with icebreaking or ship passage through brash ice. Vibration levels measured on the bow of a ship were more than 2 g during ice crushing. This indicates that the high vibration levels at

high frequencies associated with icebreaking are greatly attenuated as far as onshore vibrations are concerned. Icebreaking and opening the channel were important in reducing vibration levels by about 50% for a ship following closely behind another ship. The duration of vibrations onshore was found to be comparable to earthquake durations, 10-20 s.

The third objective, determination of the mode of energy transmission, cannot be definitely identified after only one year's study. The three modes of transmission, in the water, in the soil and in the ice, are discussed in only a qualitative manner. There is some evidence that the same vibration levels occur with a solid ice cover and with a broken cover. This suggests energy transmission via a P wave through the water, with the ice, solid or broken, acting as a waveguide and via resonant coupling between a P wave in the water and an S wave or a Rayleigh wave in the bed. There is evidence to show that considerable energy can be generated by a bow wave and transmitted under an ice cover to shore. When the velocity of a ship approaches the critical wave velocity this energy is concentrated. Vibration levels with an ice cover were about two to five times the levels with no ice cover.

Two major reasons for the low vibration levels during 1979 are that there were no ice jams in the river and the deep snow cover prevented the ground from freezing. This unfrozen ground acted to attenuate the vibration signals. In fact, a deep snow cover, natural or artificial, could be used to keep the ground unfrozen and reduce the vibration levels.

Recommended approaches in future work should include removing the snow to determine the effect of frozen ground, using a pressure transducer to determine the water wave pressure

and instrumenting the USCGC *Mackinaw* to synchronize on board and on shore signals. Other useful information could be obtained from a river seismic study, from the determination of the vectorial resultant of the three-dimensional transducer signals, and from a vibration questionnaire survey of the residents, similar to standard earthquake surveys. A larger array of transducers should be used to determine the absorption or attenuation coefficient in the ice, in the oil and in the water.

LITERATURE CITED

- Clough, R.W. and J. Penzien (1975) *Dynamics of Structures*. New York McGraw-Hill
Great Lakes Red Book, 76th ed (1979) St Clair Shore, Michigan Fourth Sea Coast Publishing Co., Inc
Harris, E. and A.D. Crede (1975) *Shock and Vibration Handbook* 2nd ed New York McGraw-Hill
National Oceanographic and Atmospheric Administration (1979) Climatological data, January 1979, Michigan Vol. 93, no 12, Asheville, N.C. NOAA
Noonan, E.F. and S. Feldman, (1978) State-of-the-art for shipboard vibration and noise control Ship Vibration Symposium, Arlington, Va., SNAME, p. A-1 to A-25
Ormondroyd, J. (1950) Investigation of structural stresses in icebreaking vessels Project M720-6, U.S. Navy Dept., Office of Naval Research
Perham, R.E. (1978) Ice and ship effects on the St. Marys River ice booms Canadian Journal of Civil Engineering, vol 5, p 222-230
Peters, A.S. (1950) The effect of a floating mat on water waves Communications on Pure and Applied Mathematics, vol 3, p 319-354
Stiansen, S.G. (1978) Propeller and wave-induced hull structure vibrations Ship Vibration Symposium, Arlington, Va., SNAME, p L-1 to L-24
White, J.E. (1965) *Seismic Waves: Radiation, Transmission and Attenuation*. New York McGraw-Hill
Wuebben, J.L. (1978) CRREL trip report—Sault Ste Marie, Michigan, 14 February 1978 U.S. Army Cold Regions Research and Engineering Laboratory

A facsimile catalog card in Library of Congress MARC format is reproduced below.

Haynes, F.D.

Vibrations caused by ship traffic on an ice-covered waterway / by F.D. Haynes and M. Määttänen. Hanover, N.H.: U.S. Army Cold Regions Research and Engineering Laboratory; Springfield, Va.: available from National Technical Information Service, 1981.

vi, 36 p., illus.; 28 cm. (CRREL Report 81-5.)

Prepared for U.S. Army Engineer District, Detroit/ by Corps of Engineers, U.S. Army Cold Regions Research and Engineering Laboratory.

Bibliography: p. 27.

1. Frequency analysis. 2. Frozen soil. 3. Ice.
4. Ice breaking. 5. Seismic waves. 6. Shipboard vibrations. 7. Vibration. I. Määttänen, M.
II. United States. Army. Corps of Engineers. III.
Army Cold Regions Research and Engineering Laboratory,
Hanover, N.H. IV. Series: CRREL Report 81-5.

